Temperature-dependent striped antiferromagnetism of LaFeAsO in a Green's function approach

2009 J. Phys.: Condens. Matter 21 195701

(http://iopscience.iop.org/0953-8984/21/19/195701)

J. Phys.: Condens. Matter **21** (2009) 195701 (6pp) doi:10.1088/0953-8984/21/19/195701

Temperature-dependent striped antiferromagnetism of LaFeAsO in a Green's function approach

Gui-Bin Liu and Bang-Gui Liu

Institute of Physics, Chinese Academy of Sciences, Beijing 100190, People's Republic of China
and
Beijing National Laboratory for Condensed Matter Physics, Beijing 100190, People's Republic of China

E-mail: gbliu@aphy.iphy.ac.cn and bgliu@aphy.iphy.ac.cn

Received 10 February 2009, in final form 30 March 2009
Published 22 April 2009
Online at stacks.iop.org/JPhysCM/21/195701

Abstract

We use a Green's function method to study the temperature-dependent average moment and magnetic phase-transition temperature of the striped antiferromagnetism of LaFeAsO, and other similar compounds, as the parents of FeAs-based superconductors. We consider the nearest and the next-nearest couplings in the FeAs layer, and the nearest coupling for inter-layer spin interaction. The dependence of the transition temperature T_N and the zero-temperature average spin on the interaction constants is investigated. We obtain an analytical expression for T_N and determine our temperature-dependent average spin from zero temperature to T_N in terms of unified self-consistent equations. For LaFeAsO, we obtain a reasonable estimation of the coupling interactions with the experimental transition temperature $T_N = 138$ K. Our results also show that a non-zero antiferromagnetic (AFM) inter-layer coupling is essential for the existence of a non-zero T_N, and the many-body AFM fluctuations reduce substantially the low-temperature magnetic moment per Fe towards the experimental value. Our Green's function approach can be used for other FeAs-based parent compounds and these results should be useful to understand the physical properties of FeAs-based superconductors.

(Some figures in this article are in colour only in the electronic version)

1. Introduction

The discovery of the high-temperature superconductor LaF_xFeAsO_{1-x} by Kamihara *et al* [1] has triggered world-wide research on all aspects of FeAs-based pnictides superconductors and their parent compounds, namely LnFeAsO (Ln = La [1–7], Ce [8, 9], Pr [10], Nd [11, 12], Sm [13–15], ...) and AFe_2As_2 (A = Ca [16–18], Sr [19–21], Ba [22, 23, 21]). LnFeAsO and AFe_2As_2 have some common characteristics: (a) they are all of layered structure and have structure transitions from high-temperature tetragonal to low-temperature orthorhombic symmetry; (b) they all have stripe-like antiferromagnetic (AFM) order formed by Fe atoms, and the AFM transition temperatures T_Ns are not higher than the structure transition temperatures T_Ss; (c) the onset of superconductivity competes with the AFM and structure transitions [24, 25], and they differ in the sense that $T_N < T_S$ for LnFeAsO and $T_N = T_S$ for AFe_2As_2. Both of the two series can be made superconducting by doping them with appropriate dopants or applying pressures. It should help in understanding the superconductivity of FeAs-based materials to elucidate the corresponding antiferromagnetism of the parent compounds.

LaFeAsO is the prototype and the representative of the parent compounds of FeAs-based superconductors, and thus we focus on the striped AFM order of undoped LaFeAsO, whose T_N is 138 K and T_S 156 K [2, 3]. First-principles results confirm that the stripe-AFM order is the magnetic ground state [5]. Spin-wave approaches were adopted to give the low-temperature excitation spectra [7, 26, 19], and the spin–orbit interaction and p–d hybridization are used to explain the

observed small magnetic moment 0.25 $\mu_B \sim 0.36\ \mu_B$ per Fe at low temperature [2, 3, 6]. However, it is highly desirable to describe the magnetic moment from zero temperature to T_N within a unified theory.

In this paper, we use a Green's function method to study the temperature-dependent average moment and phase-transition temperature of the striped antiferromagnetism of LaFeAsO, and other similar compounds, as the parents of FeAs-based superconductors. We consider the nearest and the next-nearest couplings in the FeAs layer, and only the nearest one for the inter-layer spin interaction. The dependence of the transition temperature T_N and the zero-temperature average spin on the four interactions are investigated. We obtain an analytical expression for T_N, and determine our temperature-dependent average spin from zero temperature to T_N in terms of unified self-consistent equations. For LaFeAsO, we obtain a reasonable estimation of the coupling interactions with experimental phase-transition temperature $T_N = 138$ K. Our results also show that a non-zero antiferromagnetic inter-layer coupling is essential for the existence of a non-zero T_N, and the many-body AFM fluctuations reduce substantially the low-temperature magnetic moment per Fe towards the experimental value. More detailed results will be presented. The remaining part of this paper is organized as follows. In section 2, we shall give our spin model, the Green's function derivation and our main analytical results. In section 3, we shall present our numerical results and make corresponding discussions. Our conclusion is given in section 4.

2. Effective model, Green's function derivation, and main analytical results

To deal with the striped AFM configuration of LaFeAsO, we consider the Fe lattice of the original orthorhombic LaFeAsO structure and divide it into two sublattices, in each of which the Fe spins align parallel but are antiparallel between the two sublattices (figure 1). Hence we consider an anisotropic Heisenberg Hamiltonian

$$\hat{H} = \sum_{\langle \mathbf{i},\mathbf{j}\rangle} J_{\langle \mathbf{i},\mathbf{j}\rangle} \hat{\mathbf{S}}_i \cdot \hat{\mathbf{S}}_j + J_2 \sum_{\langle\langle \mathbf{i},\mathbf{j}\rangle\rangle} \hat{\mathbf{S}}_i \cdot \hat{\mathbf{S}}_j, \tag{1}$$

in which $\hat{\mathbf{S}}_\mathbf{i}$ denotes the quantum spin operator at the lattice position $\mathbf{i}$, $\langle \mathbf{i},\mathbf{j}\rangle$ means nearest-neighbor (NN) spin pairs, and $\langle\langle \mathbf{i},\mathbf{j}\rangle\rangle$ means next-nearest-neighbor (NNN) spin pairs in the a–b plane (we only consider NNN pairs in the a–b plane because the inter-layer interactions are very weak). The NN interaction $J_{\langle \mathbf{i},\mathbf{j}\rangle}$ can be three values: J_{1a} which is the spin interaction between parallel NN spins in the a–b plane, J_{1b} between antiparallel NN spins in the a–b plane and J_c between the inter-layer NN spins. J_2 is the interaction between NNN spins in the a–b plane. Four different Js make $\hat{H}$ anisotropic. To differentiate the spin operators in SL1 and SL2, we use $\hat{\mathbf{S}}_{1\mathbf{i}}$ and $\hat{\mathbf{S}}_{2\mathbf{j}}$ to represent them, respectively. For spins in SL2, we make transformations: $\hat{S}'^z_{2\mathbf{j}} = -\hat{S}^z_{2\mathbf{j}}$, $\hat{S}'^+_{2\mathbf{j}} = \hat{S}^-_{2\mathbf{j}}$, $\hat{S}'^-_{2\mathbf{j}} = \hat{S}^+_{2\mathbf{j}}$ and then have

$$\begin{aligned}\hat{\mathbf{S}}_{1\mathbf{i}} \cdot \hat{\mathbf{S}}_{2\mathbf{j}} &= \tfrac{1}{2}(\hat{S}^+_{1\mathbf{i}}\hat{S}^-_{2\mathbf{j}} + \hat{S}^-_{1\mathbf{i}}\hat{S}^+_{2\mathbf{j}}) + \hat{S}^z_{1\mathbf{i}}\hat{S}^z_{2\mathbf{j}} \\ &= \tfrac{1}{2}(\hat{S}^+_{1\mathbf{i}}\hat{S}'^+_{2\mathbf{j}} + \hat{S}^-_{1\mathbf{i}}\hat{S}'^-_{2\mathbf{j}}) - \hat{S}^z_{1\mathbf{i}}\hat{S}'^z_{2\mathbf{j}}.\end{aligned} \tag{2}$$

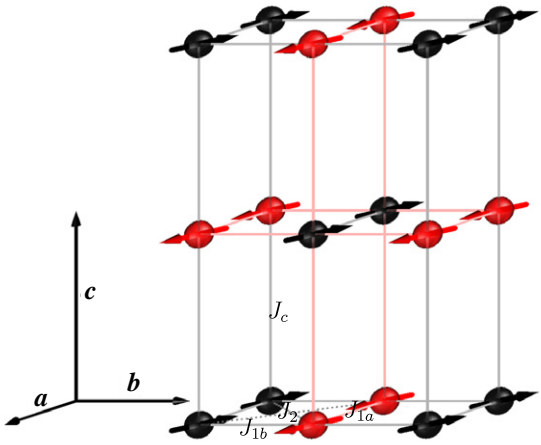

Figure 1. The magnetic cell with volume $a \times 2b \times 2c$ of the orthorhombic Fe spin lattice. The Fe lattice consists of two spin sublattices: SL1 (black) and SL2 (red or gray). $\boldsymbol{a}$ and $\boldsymbol{b}$ are the two base vectors in the FeAs layer, and $\boldsymbol{c}$ is perpendicular to both $\boldsymbol{a}$ and $\boldsymbol{b}$.

Inserting (2) into (1) we can get the Hamiltonian expressed by $\mathbf{S}_{1\mathbf{i}}$ and $\mathbf{S}'_{2\mathbf{j}}$ (simple but too long to give out here).

Accordingly, we use a Green's function method [27, 28] to solve the model (1). In this scheme one uses a double-time Green's function $\langle\langle \hat{A}(t); \hat{B}(t')\rangle\rangle$ ($\hat{A}$ and $\hat{B}$ represent two arbitrary quantum operators) which satisfies the following equation of motion:

$$\begin{aligned}\mathrm{i}\hbar \frac{\mathrm{d}}{\mathrm{d}t}\langle\langle \hat{A}(t); \hat{B}(t')\rangle\rangle &= \delta(t-t')\langle[\hat{A}(t), \hat{B}(t)]\rangle \\ &+ \langle\langle[\hat{A}(t), \hat{H}]; \hat{B}(t')\rangle\rangle.\end{aligned} \tag{3}$$

This approach proves successful for various Heisenberg spin models [27–32]. In [30], there is a detailed but somewhat long derivation about the Green's function method for Heisenberg spin models, and by considering this derivation, we conclude that the process of using Green's functions to solve the average spin of a Heisenberg model can be simplified into three steps: (a) construct Green's functions $\langle\langle \hat{S}^+_\mathbf{i}; \hat{S}^-_\mathbf{j}\rangle\rangle$ and their equations of motion via (3) and then use a Tyablikov cutoff approximation (4) to decouple the equations of motion [28];

$$\langle\langle \hat{S}^z_\mathbf{i}\hat{S}^+_\mathbf{j}; \hat{B}\rangle\rangle \xrightarrow{\mathbf{i}\neq\mathbf{j}} \langle\hat{S}^z\rangle\langle\langle \hat{S}^+_\mathbf{j}; \hat{B}\rangle\rangle \tag{4}$$

(b) use the spectrum theorem to express the correlation function $\langle\hat{S}^-\hat{S}^+\rangle$ in term of the average spin z-component $\langle\hat{S}^z\rangle$ and then obtain the $\Phi(\langle\hat{S}^z\rangle)$ function

$$\Phi(\langle\hat{S}^z\rangle) = \tfrac{1}{2}\langle\hat{S}^-\hat{S}^+\rangle/\langle\hat{S}^z\rangle; \tag{5}$$

(c) use the Callen expression (6) [30] to evaluate $\langle\hat{S}^z\rangle$ self-consistently

$$\langle\hat{S}^z\rangle = \frac{(S-\Phi)(1+\Phi)^{2S+1} + (S+1+\Phi)\Phi^{2S+1}}{(1+\Phi)^{2S+1} - \Phi^{2S+1}}. \tag{6}$$

According to the three steps given above, for our spin system we construct double-time spin Green's functions between spin operators at two positions $\mathbf{i}$ and $\mathbf{j}$ in SL1

$$\tilde{G}^{(11)}_{\mathbf{ij}}(t,t') = \langle\langle \hat{S}^+_{1\mathbf{i}}(t); \hat{S}^-_{1\mathbf{j}}(t')\rangle\rangle \tag{7}$$

and Green's functions between spin operators at two positions $\mathbf{i}'$ in SL2 and $\mathbf{j}'$ in SL1

$$\tilde{G}^{(21)}_{\mathbf{i}'\mathbf{j}'}(t,t') = \langle\langle \hat{S}^{-}_{2\mathbf{i}'}(t); \hat{S}^{-}_{1\mathbf{j}'}(t')\rangle\rangle. \tag{8}$$

Equation (7) can be expressed as a Fourier expansion

$$\tilde{G}^{(11)}_{\mathbf{ij}}(t,t') = \frac{1}{2\pi\hbar}\int G^{(11)}_{\mathbf{ij}}(\omega)\mathrm{e}^{-\mathrm{i}\omega(t-t')/\hbar}\mathrm{d}\omega, \tag{9}$$

because the Hamiltonian (1) is time independent, and (8) is similar. Assuming that each spin has the same average $\langle\hat{S}^z_1\rangle$ for SL1 and $\langle\hat{S}'^z_2\rangle$ for SL2, and because of the AFM symmetry plus the transformation (2), we have $\langle\hat{S}^z_1\rangle = \langle\hat{S}'^z_2\rangle = \langle\hat{S}^z\rangle$. Then using the Fourier transformation as shown in (9), making the Tyablikov cutoff approximation to decouple the equations of motion, and another Fourier transformation from lattice sites real space to $\mathbf{k}$ space, we have

$$1 + g^{(11)}_{\mathbf{k}}\left[J_{1b}\rho_1(\mathbf{k}) - \frac{\omega}{2\langle\hat{S}^z\rangle}\right] + J_{1b}g^{(21)}_{\mathbf{k}}\rho_2(\mathbf{k}) = 0 \tag{10}$$

and

$$g^{(11)}_{\mathbf{k}}J_{1b}\rho_2(\mathbf{k}) + g^{(21)}_{\mathbf{k}}\left[J_{1b}\rho_1(\mathbf{k}) + \frac{\omega}{2\langle\hat{S}^z\rangle}\right] = 0, \tag{11}$$

in which

$$\begin{aligned} g^{(11)}_{\mathbf{k}} &= \sum_{\mathbf{r}} G^{(11)}_{\mathbf{i},\mathbf{i}+\mathbf{r}}(\omega)\mathrm{e}^{-\mathrm{i}\mathbf{k}\cdot\mathbf{r}} \\ g^{(21)}_{\mathbf{k}} &= \sum_{\mathbf{r}} G^{(21)}_{\mathbf{i},\mathbf{i}+\mathbf{r}}(\omega)\mathrm{e}^{-\mathrm{i}\mathbf{k}\cdot\mathbf{r}}, \end{aligned} \tag{12}$$

$$\begin{aligned} \rho_1(\mathbf{k}) &= -p(1-\cos\mathbf{k}\cdot\boldsymbol{a}) + 1 + 2q + r \\ \rho_2(\mathbf{k}) &= (1 + 2q\cos\mathbf{k}\cdot\boldsymbol{a})\cos\mathbf{k}\cdot\boldsymbol{b} + r\cos\mathbf{k}\cdot\boldsymbol{c}, \end{aligned} \tag{13}$$

and

$$p \equiv \frac{J_{1a}}{J_{1b}}, \qquad q \equiv \frac{J_2}{J_{1b}}, \qquad r \equiv \frac{J_c}{J_{1b}}. \tag{14}$$

We should point out that: (a) the wavevector $\mathbf{k}$ we used here is based on the whole lattice sites (SL1 + SL2), so $\mathbf{r}$ in summations of (12) runs over all sites in the whole lattice; (b) for a homogeneous system, $G^{(11)}_{\mathbf{i},\mathbf{i}+\mathbf{r}}$ is only a function of relative position $\mathbf{r}$ and independent of $\mathbf{i}$ (as a result $G^{(11)}_{\mathbf{ii}} = G^{(11)}$ which is used below); $G^{(21)}_{\mathbf{i},\mathbf{i}+\mathbf{r}}$ is analogous.

From (10) and (11) we derive

$$g^{(11)}_{\mathbf{k}} = \frac{\langle\hat{S}^z\rangle}{\sqrt{\rho_1^2-\rho_2^2}}\left[\frac{\rho_1+\sqrt{\rho_1^2-\rho_2^2}}{\omega - E(\mathbf{k})} - \frac{\rho_1-\sqrt{\rho_1^2-\rho_2^2}}{\omega + E(\mathbf{k})}\right], \tag{15}$$

where $E(\mathbf{k})$ is the spin excitation spectrum defined by

$$E(\mathbf{k}) = 2J_{1b}\langle\hat{S}^z\rangle\sqrt{\rho_1^2(\mathbf{k}) - \rho_2^2(\mathbf{k})}. \tag{16}$$

And from $g^{(11)}_{\mathbf{k}}$ we get $G^{(11)}_{\mathbf{ij}}$

$$G^{(11)}_{\mathbf{ij}}(\omega) = \frac{1}{N}\sum_{\mathbf{k}\in\mathrm{BZ}} g^{(11)}_{\mathbf{k}}\mathrm{e}^{\mathrm{i}\mathbf{k}\cdot(\mathbf{i}-\mathbf{j})}, \tag{17}$$

in which N is the total number of spins in SL1 and SL2, and BZ denotes the first Brillouin zone (there are N $\mathbf{k}$-points in BZ). Using the spectrum theorem and letting $\mathbf{j} = \mathbf{i}$, we get the correlation function $\langle\hat{S}^-_1\hat{S}^+_1\rangle$ as follow

$$\begin{aligned} \langle\hat{S}^-_1\hat{S}^+_1\rangle &= -\frac{1}{\pi}\int_{-\infty}^{\infty}\frac{\mathrm{Im}[G^{(11)}(\omega+\mathrm{i}0^+)]}{\mathrm{e}^{\beta\omega}-1}\mathrm{d}\omega \\ &= \frac{\langle\hat{S}^z_1\rangle}{N}\sum_{\mathbf{k}\in\mathrm{BZ}}\left[\frac{\rho_1}{\sqrt{\rho_1^2-\rho_2^2}}\coth\frac{\beta E(\mathbf{k})}{2} - 1\right], \end{aligned} \tag{18}$$

where $\beta = 1/(k_\mathrm{B}T)$, T is temperature, and k_B is the Boltzmann constant. Then using (5) we get the Φ function:

$$\Phi(\langle\hat{S}^z\rangle) = \frac{1}{2N}\sum_{\mathbf{k}\in\mathrm{BZ}}\left[\frac{\rho_1}{\sqrt{\rho_1^2-\rho_2^2}}\coth\frac{\beta E(\mathbf{k})}{2} - 1\right]. \tag{19}$$

Now, the average spin z-component $\langle\hat{S}^z\rangle$ can be obtained easily by self-consistently solving (19) and (6). A special case is that when the temperature $T = 0$, $\coth\frac{\beta E(\mathbf{k})}{2} \to 1$, and we have

$$\Phi_0 \equiv \Phi|_{T=0} = \frac{1}{2N}\sum_{\mathbf{k}\in\mathrm{BZ}}\left[\frac{\rho_1}{\sqrt{\rho_1^2-\rho_2^2}} - 1\right]. \tag{20}$$

At this time, Φ_0 is no longer dependent on $\langle\hat{S}^z\rangle$ and the zero-temperature average spin z-component $\langle\hat{S}^z\rangle_0$ can be obtained directly by inserting (20) into (6).

While the temperature approaches T_N, $\langle\hat{S}^z\rangle$ approaches zero and, further, $E(\mathbf{k}) \to 0$ and $\Phi \to \infty$. Expanding (19) and (6), we derive

$$\langle\hat{S}^z\rangle \propto \sqrt{1 - \frac{T}{T_\mathrm{N}}}, \tag{21}$$

where T_N is defined by

$$T_\mathrm{N} = \frac{2J_{1b}S(S+1)}{3\Gamma k_\mathrm{B}} \tag{22}$$

and $\Gamma = \frac{1}{N}\sum_{\mathbf{k}}[\rho_1/(\rho_1^2-\rho_2^2)]$.

3. Numerical results and discussions

There is no consensus on the magnitudes of the coupling interactions J_{1a}, J_{1b}, J_2 and J_c in FeAs-based pnictides, and many authors only consider two or three of them [4, 5, 33, 23, 19, 16, 34]. Yildirim's first-principles results show that $J_1 \sim J_2$ [5]. However, we prefer the opinion that J_{1a}, J_{1b} and J_2 originate from the AFM superexchange through As atoms [35–37]. From the viewpoint of the structure of FeAs layers, both J_{1a} and J_{1b} are mediated by two Fe–As–Fe paths (figure 2(a)) and this should mean $J_{1a} \neq J_{1b}$, but $J_{1a} \sim J_{1b}$ due to the small structural change from tetragonal to orthorhombic symmetry. J_2 is mediated by only one Fe–As–Fe path (figure 2(a)) and this should give $2J_2 \sim J_{1a}$. From the viewpoint of classical favorable energy in forming stripe-like

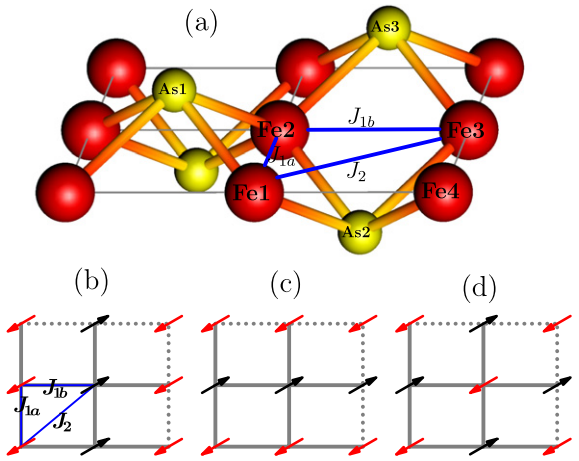

Figure 2. (a) Structure of the FeAs layer and scheme for the exchange interactions mediated by Fe–As–Fe paths: Fe1–As1–Fe2 and Fe1–As2–Fe2 for J_{1a}, Fe2–As2–Fe3 and Fe2–As3–Fe3 for J_{1b}, and Fe1–As2–Fe3 for J_2. Different AFM configurations are shown: (b) stripe-AFM along the $\boldsymbol{a}$ direction, (c) stripe-AFM along the $\boldsymbol{b}$ direction, and (d) checkerboard AFM. Energies of the three AFM configurations are given in (23).

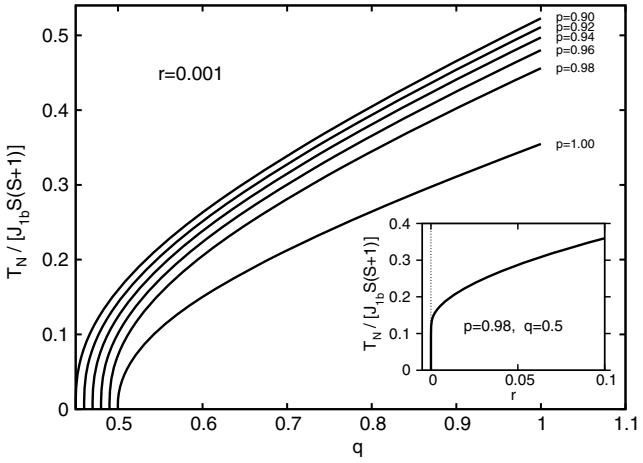

Figure 3. The reduced AFM transition temperatures $(T_N/[J_{1b}S(S+1)])$ as functions of q for $r = 0.001$ and $p = 0.90, 0.92, \ldots, 1.0$ (from top to bottom). The inset shows an r dependence of T_N for $p = 0.98$ and $q = 0.5$.

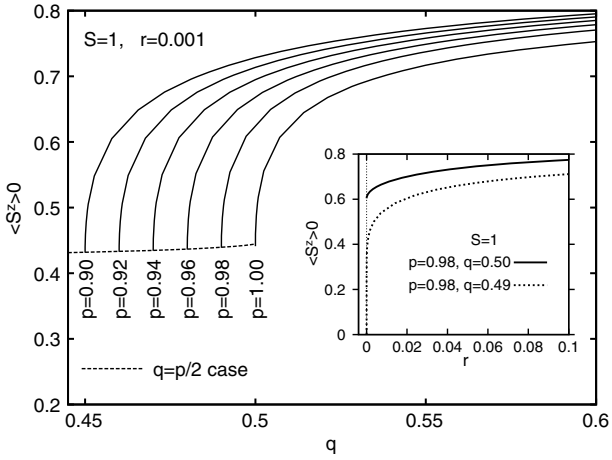

Figure 4. The zero-temperature average spins $\langle\hat{S}^z\rangle_0$ as functions of q for $r = 0.001$ and different p values: $0.90, 0.92, \ldots, 1.0$. The lower limits of $\langle\hat{S}^z\rangle_0$ are shown by the dotted line. The inset shows $\langle\hat{S}^z\rangle_0 \sim r$ curves for $(p, q) = (0.98, 0.50)$ (solid) and $(0.98, 0.49)$ (dotted), respectively.

AFM patterns along the $\boldsymbol{a}$ direction, as shown in figure 2(b) (see figures 2(b)–(d) and (23)), we have,

$$\begin{aligned} E_{(b)} &= 4J_{1a}S^2 - 4J_{1b}S^2 - 8J_2S^2 \\ E_{(c)} &= -4J_{1a}S^2 + 4J_{1b}S^2 - 8J_2S^2 \\ E_{(d)} &= -4J_{1a}S^2 - 4J_{1b}S^2 + 8J_2S^2 \ . \\ E_{(b)} < E_{(c)} &\Longrightarrow J_{1a} < J_{1b} \\ E_{(b)} < E_{(d)} &\Longrightarrow 2J_2 > J_{1a} \end{aligned} \tag{23}$$

This should mean $J_{1a} < J_{1b}$ and $2J_2 > J_{1a}$, which in fact are just the conditions that fulfil $\rho_1^2 - \rho_2^2 \geqslant 0$ to make $E(\mathbf{k})$ in (16) meaningful. As for J_c, it is a very weak long-range AFM interaction whose origin is unclear except for the superexchange. Therefore, in terms of p, q, r in (14), we confine the coupling interactions as follows:

$$\begin{aligned} &1 \geqslant p \geqslant 1 - \delta_p \\ &p/2 < q \leqslant p/2 + \delta_q, \qquad 0 < r \leqslant \delta_r \end{aligned} \tag{24}$$

where δ_p, δ_q, and δ_r are the confine parameters for p, q, and r, respectively, and they fulfil $0 < \delta_p, \delta_q, \delta_r \ll 1$. The lhs of (24) represents the necessary conditions for forming striped AFM ordering along the $\boldsymbol{a}$ direction, and the rhs the conditions for limiting p, q and r within small regions.

From figure 3 we can see that T_N increases as q and r increase but decreases as p increases. It is easy to understand. NNN spins and inter-layer NN spins all align antiparallel, so bigger AFM coupling interactions will lower the system's energy, stabilize the AFM configuration and hence enhance T_N; in contrast, spins along the $\boldsymbol{a}$ direction align parallel but have AFM interactions, therefore a bigger p will increase the system's energy, destabilize the AFM configuration and hence decrease T_N. Note that while $q \to p/2$ or $r \to 0$, $T_N \to 0$, that is to say, both the existence of an AFM inter-layer interaction J_c and the condition $2J_2 > J_{1a}$ are essential to form striped AFM ordering. In fact, when $r = 0$ this system becomes two-dimensional, and the result of $T_N = 0$ in two-dimensions is analogous to the Mermin–Wagner theorem for isotropic interactions [38]. We also see that the critical condition $p = 1$ does not lead to $T_N \to 0$, which shows that $J_{1a} = J_{1b}$ is not a fatal factor to kill T_N but only a critical value to separate the two cases shown in figures 2(b) and (c).

The magnetic moment per Fe of LaFeAsO at low temperature is reported experimentally as 0.36 μ_B [2] or 0.25 μ_B [3], both of which are very small compared to the first-principles values 2.2–2.4 μ_B/Fe [39, 40]. Accordingly, we choose $S = 1$ in our model (assuming the Landé g-factor equals 2). Figure 4 shows the zero-temperature average spin $\langle\hat{S}^z\rangle_0$. Similar to T_N, $\langle\hat{S}^z\rangle_0$ is also an increasing function

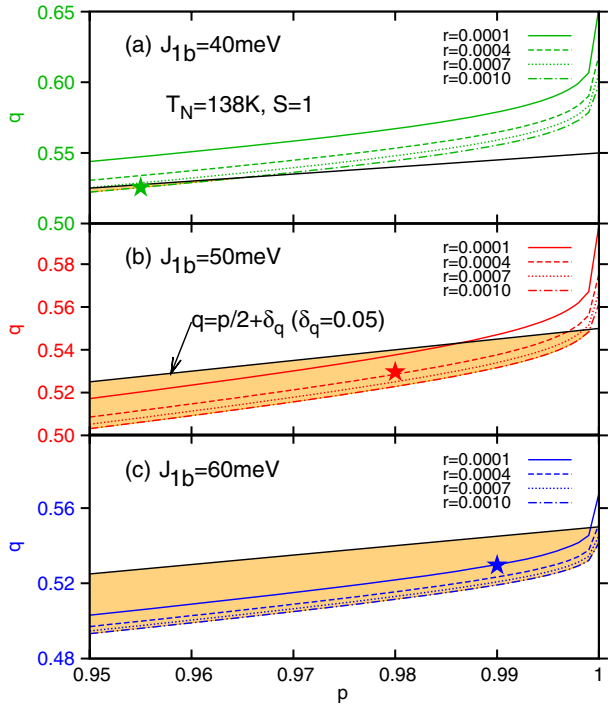

Figure 5. The parameter regions (orange or gray) satisfying (24) with $T_N = 138$ K for (a) $J_{1b} = 40$ meV, (b) $J_{1b} = 50$ meV and (c) $J_{1b} = 60$ meV, where we use $\delta_p = 0.05$, $\delta_q = 0.05$ and $\delta_r = 0.001$. The star shows the value $(p, q, r) = (0.955, 0.526, 0.0009)$ in (a), $(0.98, 0.53, 0.0003)$ in (b), or $(0.99, 0.53, 0.0001)$ in (c).

Table 1. $J_{1b}^{\min}$ for given δ_p, δ_q and δ_r.

δ_q	δ_r	δ_p	$J_{1b}^{\min}$ (meV)
0.01	0.0001	0.01	104.4
		0.1	89.8
	0.001	0.01	87.1
		0.1	72.6
0.05	0.0001	0.01	50.9
		0.1	44.6
	0.001	0.01	43.6
		0.1	37.2

of both q and r but a decreasing function of p. However, $\langle\hat{S}^z\rangle_0 \to 0$ only when both $r \to 0$ and $q \to p/2$. When only $r \to 0$ or $q \to p/2$ is met, $\langle\hat{S}^z\rangle_0$ approaches a minimum but not zero, while at the same time $T_N \to 0$.

There are four Js in our model. What are their values? Let us have a look at what they can be under the condition $T_N = 138$ K. Figure 5 shows the regions available for p, q and r under conditions (24), with $\delta_p = 0.05$, $\delta_q = 0.05$ and $\delta_r = 0.001$, in orange (gray) color for $J_{1b} = 40$ meV, 50 meV, and 60 meV, respectively. The smaller J_{1b}, the smaller the parameter region available. Hence, for given δ_p, δ_q and δ_r, there is a lower limit for J_{1b} to fulfil a given T_N. This lower limit, written as $J_{1b}^{\min}$, is given in table 1, which shows that the smaller each of δ_p, δ_q and δ_r is, the bigger $J_{1b}^{\min}$ is. However, although no upper limit for J_{1b} is given, J_{1b} cannot be infinitely large. In fact, first-principles results show that $J_{1b} \sim 50$ meV [4, 33].

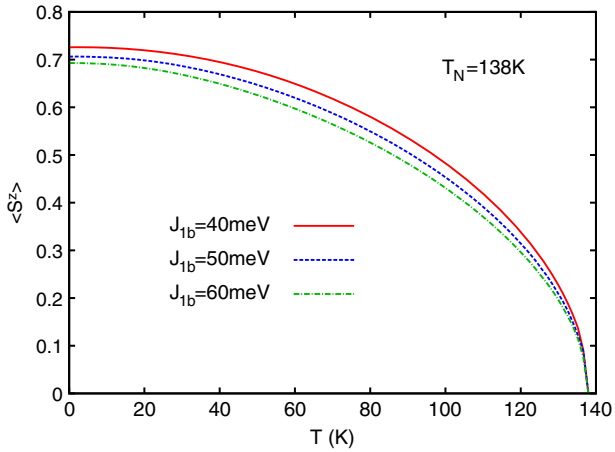

Figure 6. The average spins $\langle\hat{S}^z\rangle$ as functions of the temperature T for $J_{1b} = 40$, 50 and 60 meV. The corresponding (p, q, r) parameters are (0.955, 0.526, 0.0009), (0.98, 0.53, 0.0003) and (0.99, 0.53, 0.0001), respectively.

Table 2. AFM and structure transition temperatures T_N and T_S of LnFeAsO.

Ln	La	Ce	Pr	Nd	Sm
T_N (K)	138	140	127	141	140
T_S (K)	156	155	153	—	—
Reference	[3]	[8]	[10]	[11]	[41]

Here we did not use the experimental data for the low-temperature magnetic moment per Fe atom, which amounts to $\langle\hat{S}^z\rangle_0 = 0.13$–$0.18$, to determine the Js, because it is too small. If $\langle\hat{S}^z\rangle_0 = 0.18$ is met, we must have $\delta_r < 10^{-6}$, even if $q = p/2$ is taken to minimize $\langle\hat{S}^z\rangle_0$ (see inset of figure 4). Such a tiny r definitely cannot fall within the orange (gray) area in figure 5 with a reasonable J_{1b} to fulfil $T_N = 138$ K. That is to say, although the many-body AFM fluctuations substantially reduce the low-temperature magnetic moment per Fe, they cannot be in full charge of the very small low-temperature magnetic moment which indeed is also ascribed to spin–orbit and p–d hybridization etc [6].

We choose three sets of Js from the regions available in figure 5 for estimation (the three stars): $(p, q, r) = (0.955, 0.526, 0.0009)$, $(0.98, 0.53, 0.0003)$, and $(0.99, 0.53, 0.0001)$, for $J_{1b} = 40$ meV, 50 meV, and 60 meV, respectively. In terms of J_{1b}, J_{1a}, J_2 and J_c, we can refer to them as $J_{1b} = 50 \pm 10$ meV, $J_{1a} = 49 \pm 10$ meV, $J_2 = 26 \pm 5$ meV, and $J_c = 0.020 \pm 0.015$ meV. The average spin $\langle\hat{S}^z\rangle$ versus temperature T curves with the three sets of parameters given above are shown in figure 6.

We take LaFeAsO as an example here, however our calculations are not restricted to LaFeAsO, because nearly all LnFeAsO have similar or even the same transition temperatures (see table 2). It seems that T_N does not vary much with different Ln. This is in contrast to AFe_2As_2, whose T_N varies with A: $T_N = 172.5$ K [18] for A = Ca; $T_N = 198$ K [20], 205 K [42] or 220 K [43] for A = Sr and $T_N = 140$ K [22] or 135 K [44] for A = Ba. Although there are some differences of structure between LnFeAsO and AFe_2As_2,

we believe that our model works well for both of them, because they both have layered structures with stripe-like AFM order formed by Fe atoms. Indeed, this can also be extended to Fe(SeTe) [45, 46], which has nearly the same properties and can be superconducting under certain conditions.

4. Conclusion

In summary, we use a Green's function method to study the striped AFM order formed by Fe atoms in LnFeAsO which is a representative of the parent compounds of recently discovered Fe-based superconductors. We take LaFeAsO as the example to analyze the AFM transition temperature T_N and zero-temperature average spin $\langle\hat{S}^z\rangle_0$, and show that both T_N and $\langle\hat{S}^z\rangle_0$ are increasing functions of J_{1b}, J_2 and J_c but decreasing functions of J_{1a}. By using $T_N = 138$ K, we make a reasonable estimation of the coupling interactions, $J_{1b} = 50 \pm 10$ meV, $J_{1a} = 49 \pm 10$ meV, $J_2 = 26 \pm 5$ meV, and $J_c = 0.020 \pm 0.015$ meV. The average spin $\langle\hat{S}^z\rangle$ is determined in the same way from zero temperature to T_N, and T_N is expressed analytically. Our results also show that a non-zero AFM inter-layer coupling J_c is essential for the existence of a non-zero T_N and that the AFM fluctuations substantially reduce the low-temperature magnetic moment towards the small experimental value. Although our results cannot determine the relations between structure and AFM transitions, we believe that the AFM transition is most likely caused by the structure transition, because most of the experimental results show $T_N \leqslant T_S$ for FeAs-based pnictides. Our Green's function approach to the striped AFM properties can be used for other FeAs-based parent compounds.

Acknowledgments

This work is supported by the Nature Science Foundation of China (Grant Nos 10874232 and 10774180), by the Chinese Academy of Sciences (Grant No. KJCX2.YW.W09-5), and by the Chinese Department of Science and Technology (Grant No. 2005CB623602).

References

[1] Kamihara Y, Watanabe T, Hirano M and Hosono H 2008 *J. Am. Chem. Soc.* **130** 3296
[2] de la Cruz C *et al* 2008 *Nature* **453** 899
[3] Klauss H H *et al* 2008 *Phys. Rev. Lett.* **101** 077005
[4] Yin Z P, Lebègue S, Han M J, Neal B P, Savrasov S Y and Pickett W E 2008 *Phys. Rev. Lett.* **101** 047001
[5] Yildirim T 2008 *Phys. Rev. Lett.* **101** 057010
[6] Wu J, Phillips P and Castro Neto A H 2008 *Phys. Rev. Lett.* **101** 126401
[7] Fang C, Yao H, Tsai W F, Hu J P and Kivelson S A 2008 *Phys. Rev.* B **77** 224509
[8] Zhao J *et al* 2008 *Nat. Mater.* **7** 953
[9] Chen G F, Li Z, Wu D, Li G, Hu W Z, Dong J, Zheng P, Luo J L and Wang N L 2008 *Phys. Rev. Lett.* **100** 247002
[10] Zhao J *et al* 2008 *Phys. Rev.* B **78** 132504
[11] Chen Y, Lynn J W, Li J, Li G, Chen G F, Luo J L, Wang N L, Dai P, dela Cruz C and Mook H A 2008 *Phys. Rev.* B **78** 064515
[12] Jia Y, Cheng P, Fang L, Luo H, Yang H, Ren C, Shan L, Gu C and Wen H H 2008 *Appl. Phys. Lett.* **93** 032503
[13] Chen X H, Wu T, Wu G, Liu R H, Chen H and Fang D F 2008 *Nature* **453** 761
[14] Ding L, He C, Dong J K, Wu T, Liu R H, Chen X H and Li S Y 2008 *Phys. Rev.* B **77** 180510(R)
[15] Drew A J *et al* 2008 *Phys. Rev. Lett.* **101** 097010
[16] McQueeney R J *et al* 2008 *Phys. Rev. Lett.* **101** 227205
[17] Torikachvili M S, Bud'ko S L, Ni N and Canfield P C 2008 *Phys. Rev. Lett.* **101** 057006
[18] Goldman A I, Argyriou D N, Ouladdiaf B, Chatterji T, Kreyssig A, Nandi S, Ni N, Bud'ko S L, Canfield P C and McQueeney R J 2008 *Phys. Rev.* B **78** 100506(R)
[19] Zhao J *et al* 2008 *Phys. Rev. Lett.* **101** 167203
[20] Yan J Q *et al* 2008 *Phys. Rev.* B **78** 024516
[21] Hu W Z, Dong J, Li G, Li Z, Zheng P, Chen G F, Luo J L and Wang N L 2008 *Phys. Rev. Lett.* **101** 257005
[22] Rotter M, Tegel M, Johrendt D, Schellenberg I, Hermes W and Pöttgen R 2008 *Phys. Rev.* B **78** 020503(R)
[23] Ewings R A, Perring T G, Bewley R I, Guidi T, Pitcher M J, Parker D R, Clarke S J and Boothroyd A T 2008 *Phys. Rev.* B **78** 220501(R)
[24] Qiu Y *et al* 2008 *Phys. Rev.* B **78** 052508
[25] Pfuner F, Analytis J G, Chu J H, Fisher I R and Degiorgi L 2008 arXiv:0811.2195v1 [cond-mat]
[26] Yao D X and Carlson E W 2008 *Phys. Rev.* B **78** 052507
[27] Bogoliubov N N and Tyablikov S V 1959 *Dokl. Akad. Nauk SSSR* **126** 53
[28] Tyablikov S V 1959 *Ukr. Mat. Zh.* **11** 287
[29] Tahir-Kheli R A and ter Haar D 1962 *Phys. Rev.* **127** 88
[30] Callen H B 1963 *Phys. Rev.* **130** 890
[31] Liu B G 1990 *Phys. Rev.* B **41** 9563
[32] Liu B G and Pu F C 2001 *J. Magn. Magn. Mater.* **231** 307
[33] Ma F, Lu Z Y and Xiang T 2008 *Phys. Rev.* B **78** 224517
[34] Yaresko A N, Liu G Q, Antonov V N and Andersen O K 2008 arXiv:0810.4469v1 [cond-mat]
[35] Si Q and Abrahams E 2008 *Phys. Rev. Lett.* **101** 076401
[36] Jishi R A and Alyahyaei H M 2008 arXiv:0811.2716v1 [cond-mat]
[37] Belashchenko K D and Antropov V P 2008 *Phys. Rev.* B **78** 212515
[38] Mermin N D and Wagner H 1966 *Phys. Rev. Lett.* **17** 1133
[39] Ma F and Lu Z Y 2008 *Phys. Rev.* B **78** 033111
[40] Yildirim T 2009 *Phys. Rev. Lett.* **102** 037003
[41] Martinelli A *et al* 2008 *Supercond. Sci. Technol.* **21** 095017
[42] Kumar M, Nicklas M, Jesche A, Caroca-Canales N, Schmitt M, Hanfland M, Kasinathan D, Schwarz U, Rosner H and Geibel C 2008 *Phys. Rev.* B **78** 184516
[43] Zhao J, Ratcliff W II, Lynn J W, Chen G F, Luo J L, Wang N L, Hu J and Dai P 2008 *Phys. Rev.* B **78** 140504(R)
[44] Kitagawa K, Katayama N, Ohgushi K, Yoshida M and Takigawa M 2008 *J. Phys. Soc. Japan* **77** 114709
[45] Mizuguchi Y, Tomioka F, Tsuda S, Yamaguchi T and Takano Y 2008 *Appl. Phys. Lett.* **93** 152505
[46] Chen G F, Chen Z G, Dong J, Hu W Z, Li G, Zhang X D, Zheng P, Luo J L and Wang N L 2008 arXiv:0811.1489v1 [cond-mat]